

Neutral Triplet Collective Mode in Doped Graphene

M. Ebrahimkhas,¹ S. A. Jafari,^{2,3} and G. Baskaran⁴

¹Department of Science, Tarbiat Modarres University, Tehran 14115-175, Iran

²Department of Physics, Isfahan University of Technology, Isfahan 84156-83111, Iran

³School of Physics, Institute for Research in Fundamental Sciences (IPM), Tehran 19395-5531, Iran

⁴Institute of Mathematical Sciences, Chennai 600113, India

Particle-hole continuum in Dirac sea of graphene has an unique window. It has been predicted to support a long lived neutral triplet gapless bosonic mode that disperses over a wide energy range in the whole Brillouin zone [Phys. Rev. Lett. **89**, 016402 (2002)]. In this work, using a repulsive Hubbard model, we study the fate of such collective mode at zero temperature, in a single layer of graphene doped with electrons or holes. Doping modifies the particle-hole continuum and creates additional windows. Neutral spin-1 collective mode survives and acquires a gap that increases with doping. It is almost dispersion-less inside the new window. We suggest that the spin gap signals emergence of short range singlet correlations and a superconducting ground state for doped graphene, supporting a recent suggestion of Pathak, *et al.* [arXiv:0809.0244v1].

PACS numbers: 71.10.Fd, 72.15.Nj, 71.10.Li

I. INTRODUCTION

Graphene, a single atomic layer of graphite was the first realization of a two dimensional elemental metallic structure¹. The salient feature in the electronic spectrum of graphene, which differentiates it from other materials, is the presence of Dirac cones in its dispersion^{2,3,4}, which provides a laboratory to test relativistic type phenomena in the \sim eV energy scale. The cone-like spectrum protects the system from impurity scattering⁵, as well as many-body interactions⁶, both in normal^{7,8} and superconducting phases⁹. Because of the robust cone like dispersion with a large Fermi velocity, in graphene one observes phenomena such as quantum Hall effect¹⁰, which appear only at low temperatures and for very pure samples in standard 2D electron gas systems, to survive even at ambient temperatures. The high mobility of carriers in graphene at room temperature which is not appreciably different from its value at the liquid-helium temperature^{10,11} is another promising property of graphene for device applications. Stacking the graphene with further layers produces graphene multi-layers, such as bilayer, etc. For few layers, due to quantum size effect, the cone like dispersion is replaced by other types of chiral dispersions⁴. However, when the number of stacks is large enough (\sim 10) to approach the bulk limit of graphite, the cone like dispersion is again recovered¹², except for small electron-hole pockets at very low-energies \sim 40 meV. Therefore the phenomena driven by the Dirac nature of carriers is common in graphene and graphite^{13,14,15,16,17,18,19}. It should also be shared with the recently fabricated multi-layer epitaxial graphene²⁰.

After the pioneering work of Wallace¹² on the tight binding band picture for the electronic structure of pure and undoped graphene and graphite, it has become popular to take into account the effects of disorder, interactions and doping on top a band picture⁴. Nevertheless, there exists an alternate quantum chemical approach to the electronic properties of graphene. More than half a century ago, Pauling argued that the ground state of graphene can be described as a natural extension of the resonating valence bond (RVB) state of benzene^{21,22,23}, by totally ignoring unbound polar (charge fluctuation) configura-

tions. This overemphasize on neutral configuration makes graphene a Mott insulator. But graphene and graphite are both semi metals in reality. Since then both band aspect and Pauling's singlet correlations have been argued to be present in graphene and two important consequences have been brought theoretically. One of them is existence of gapless neutral triplet bosonic mode^{16,17} for neutral graphene, which was interpreted as a two-spinon bound excited state in a long-range RVB state. The other is a suggestion of high temperature superconductivity in doped graphene^{24,25} and other exotic superconducting states^{26,27}. An insulating RVB state is found to be stabilized²⁸ at least in the Mott insulating side of the phase diagram⁶. There is a lattice gauge theory simulation of 2 + 1 dimensional QED which predicts the critical value of the "fine structure" constant in graphene can be crossed for graphene in vacuum²⁹. In this scenario, the ground state of graphene in vacuum is expected to be a Mott insulator.

After the initial success with fabrication of undoped graphene, it has become possible to dope the Dirac sea with electrons/holes by applying appropriate gate voltage⁴. One can also cover a graphene layer with metal atoms in order to supply chemical doping of electrons/holes into the Dirac sea without significantly modifying their cone-like nature³⁰. Motivated by possibility of doping the Dirac cone, in this work we extend our earlier studies to the case of doped Dirac cone. We start with the tight-binding model. We employ the RPA approximation to analyze the particle-hole scattering processes in the triplet channel. The bi-partite nature of honeycomb lattice implies that the nearest neighbor tight-binding Hamiltonian considered in our model is particle-hole symmetric. Hence doping with electrons and holes are treated on the same footing. Therefore here we focus only on the case of electron doping. Populating the conduction band of the Dirac cone with electrons modifies the particle-hole continuum (PHC) by adding a small 2D-like portion and creating small triangular windows around the Γ and K points of the Brillouin zone, shown in Fig. 1 (c,d,e). This leads to the gap in the dispersion of the spin-1 collective mode. The dispersion of the collective mode in this window is schematically drawn with red pen in Fig. 1 (e). The gaped nature of this collective mode in doped

graphene in our RVB interpretation translates into the transformation of long range RVB state of undoped graphene²⁸ to an RVB state with shorter bonds when the Dirac cone is doped.

This paper is organized as follows: In the next section we introduce the model and the RPA formulation. Then we present the intensity plots of the RPA susceptibility showing the dispersion of the neutral triplet collective mode. In the small q limit where we use a linearized Dirac theory around the K points we obtain closed form expressions for the susceptibility. However, the numerical results are valid for the whole BZ. We end the paper with a summary and discussions.

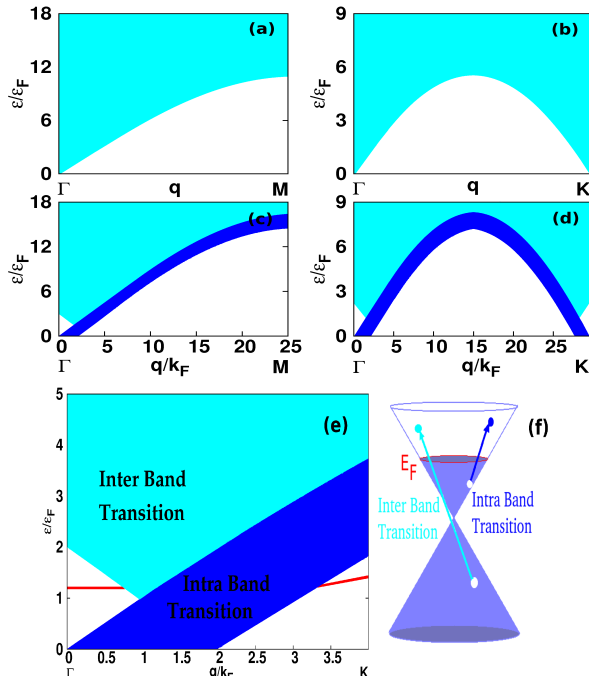


FIG. 1: (Color online) Particle-hole continuum of graphene band structure along important directions of the Brillouin zone. (a) and (b) denote the PHC for undoped graphene, while (c) and (d) correspond to doped graphene. For better comparison, the energies of both doped and undoped cases are reported in units of ε_F . In this figure, we have $\mu = \varepsilon_F = 0.5$ eV. Panel (e) is the same as (c) enlarged for clarity, which also schematically shows the neutral spin-1 collective mode branch. Panel (f) schematically depicts the cone-like band picture with two possible sets of inter-band and intra-band processes shown by cyan and blue arrows, respectively. As can be seen in (f), doping with electrons have two effects: One is to Pauli block some of the inter-band transitions which depletes the region of momenta around the Γ and K points, compared to undoped case. Second is to add a new 2D like portion to the PHC corresponding to intra-band particle-hole excitations denoted by blue in panel (e). Hence the triangular windows around Γ and K points are produced.

II. FORMULATION OF THE PROBLEM

As in our earlier works^{16,17,18} we study the spin physics which involves spin flip (triplet) processes, by focusing on the short range part of the interactions on the honeycomb lattice.

Hence the model we use is the Hubbard model defined as,

$$H = -t \sum_{\langle i,j \rangle, \sigma} (c_{i\sigma}^\dagger c_{j\sigma} + \text{h.c.}) + U \sum_j n_{j\downarrow} n_{j\uparrow}, \quad (1)$$

where i, j denote lattice sites of a honeycomb lattice, and σ stands for the spin of electrons. The spectrum of the band limit, $U = 0$, is given by $\varepsilon_{\vec{k}}^\lambda = \pm \varepsilon_{\vec{k}}$ corresponding to $\lambda = c, v$ for conduction and valence bands, respectively, with,

$$\varepsilon_{\vec{k}} = t \sqrt{1 + \cos(\sqrt{3}k_y/2) \cos(k_x/2) + 4 \cos^2(k_x/2)}, \quad (2)$$

where $t \sim 2.8$ eV is the hopping amplitude. The lattice parameter a is taken as carbon-carbon distance.

In this model, U is the on-site Coulomb repulsion. Although the bare value of U in graphene is $\sim 4t - 5t$, but within the RPA one should not increase U above $U_c \sim 2.23t$ ¹⁷. The underestimation of U_c is a known artifact of RPA, as in the sense of Hubbard-Stratonovich transformation, the RPA approximation belongs to the family of mean field approximations³¹. Therefore to be consistent in applying the RPA approximation, we restrict ourselves to values of $U \sim 2t$.

We implement the RPA approximation in the triplet particle-hole channel, which is given by³²,

$$\chi_{\text{triplet}}^{\text{RPA}}(\vec{q}, \omega) = \frac{\chi^{(0)}(\vec{q}, \omega)}{1 - U \chi^{(0)}(\vec{q}, \omega)}. \quad (3)$$

Note that the sign of U for triplet and singlet channels is different. Hence, when the above triplet susceptibility diverges, the contribution of the singlet channel to the total susceptibility will remain finite. The retarded bare susceptibility $\chi^{(0)}$ is given by the standard particle-hole form,

$$\chi^{(0)}(\vec{q}, \omega) = \frac{1}{N} \sum_{\lambda} \sum_{\vec{k}} \frac{f_{c, \vec{k}+\vec{q}} - f_{\lambda \vec{k}}}{\hbar\omega - (\varepsilon_{\vec{k}+\vec{q}}^c - \varepsilon_{\vec{k}}^\lambda) + i0^+}, \quad (4)$$

where N is the number of unit cells, and $\lambda = c, v$ stands for conduction and valence bands, respectively. Here $f_{\lambda, \vec{k}}$ is the Fermi distribution function, which determines the occupation of the state characterized with quantum labels (λ, \vec{k}) and energy $\varepsilon_{\vec{k}}^\lambda$. At $T = 0$, and for electron doping case corresponding to $\mu > 0$, the conduction band is partially occupied; i.e. from Dirac point to the Fermi level. So there are two types of particle-hole excitations: (A) *intra-band transition* corresponding to $\lambda = c$. (B) *inter-band transitions* corresponding to $\lambda = v$ of the above summation. The numerical calculation of $\chi^{(0)}(\vec{q}, \omega)$ for arbitrary \vec{q} in the BZ is straightforward. However, for the low-energy part of the spectrum where the Dirac dispersion $\varepsilon_{\vec{k}} = \hbar v_F |\vec{k}|$ governs the kinetic energy, one can obtain closed form formulae for the inter-band and intra-band parts of the susceptibility. Therefore in the following we further simplify the expressions to proceed with numerical evaluation of the integrals, as well as the analytical calculations, the details of which is presented in the appendix.

A. Intra-band term

The nature of PHC is shown in Fig. 1 (e). The part of PHC shown in blue corresponds to intra-band particle-hole processes. As can be seen this part is qualitatively similar to the PHC of standard 2D metals with extended Fermi surface. The only difference is in the form of dispersion which unlike ordinary metals with quadratic dispersion, here one has cone like dispersion. For intra-band particle-hole excitations one has:

$$\chi_{\text{intra}}^{(0)}(\vec{q}, \omega) = \frac{1}{N} \sum_{\vec{k}} \frac{f_{c, \vec{k}+\vec{q}} - f_{c, \vec{k}}}{\hbar\omega - (\epsilon_{\vec{k}+\vec{q}} - \epsilon_{\vec{k}}) + i0^+}. \quad (5)$$

In the $T \rightarrow 0$ where,

$$f_{c, \vec{k}+\vec{q}} = \frac{1}{e^{\beta(\epsilon_{\vec{k}+\vec{q}} - \mu)} + 1} \rightarrow \Theta(\mu - \epsilon_{\vec{k}+\vec{q}}), \quad (6)$$

$$f_{c, \vec{k}} = \frac{1}{e^{\beta(\epsilon_{\vec{k}} - \mu)} + 1} \rightarrow \Theta(\mu - \epsilon_{\vec{k}}), \quad (7)$$

we get,

$$\chi_{\text{intra}}^{(0)}(\vec{q}, \omega) = \frac{1}{N} \sum_{\vec{k}} \frac{\Theta(\mu - \epsilon_{\vec{k}+\vec{q}}) - \Theta(\mu - \epsilon_{\vec{k}})}{\hbar\omega - (\epsilon_{\vec{k}+\vec{q}} - \epsilon_{\vec{k}}) + i0^+}. \quad (8)$$

In the first step function we apply a change of variable $\vec{k} + \vec{q} \rightarrow -\vec{k}$, and after converting the summation to integral, we obtain:

$$\chi_{\text{intra}}^{(0)}(\vec{q}, \omega) = \frac{A}{4\pi^2} \int dk^2 \left(\frac{\Theta(k_F - k)}{\hbar\omega - (\epsilon_{\vec{k}} - \epsilon_{\vec{k}+\vec{q}}) + i0^+} - \frac{\Theta(k_F - k)}{\hbar\omega - (\epsilon_{\vec{k}+\vec{q}} - \epsilon_{\vec{k}}) + i0^+} \right), \quad (9)$$

where $A = 3\sqrt{3}a^2/2$ is the unit cell area. In the analytic calculations we use $\epsilon_{\vec{k}} = \hbar v_F |\vec{k}|$ which is valid for low energies. Therefore in analytic calculations, we will be interested in $|\vec{q}| < k_F$ region, where \vec{q} is the deviation of momentum from Γ (or K) point. Since the calculation of the above integral is standard exercise in mathematical physics, the details of the calculation of imaginary and real part of $\chi_{\text{intra}}^{(0)}$ is given in the appendix. The final results are given in Equations (A6) and (A8). These results are valid for small $|\vec{q}|$. For arbitrary \vec{q} we evaluate the integrals with numerical quadratures.

B. Inter-band term

Inter-band particle-hole excitations in undoped graphene can have any energy from zero up to a maximum value determined by the shape of band structure. But in the case of doped graphene, the inter-band particle-hole excitations of very low energy (near Γ and K points) are Pauli blocked. Hence in Fig. 1 the low-energy part of the PHC of undoped graphene (Fig. 1 a, b) is depleted to give the PHC of Fig. 1 (c,d) which is enlarged in (e). For the inter-band processes one has,

$$\chi_{\text{inter}}^{(0)}(\vec{q}, \omega) = \frac{1}{N} \sum_{\vec{k}} \frac{f_{c, \vec{k}+\vec{q}} - f_{v, \vec{k}}}{\hbar\omega - (\epsilon_{\vec{k}+\vec{q}} + \epsilon_{\vec{k}}) + i0^+}, \quad (10)$$

which in an analogous way to Eq. (9) simplifies to,

$$\chi_{\text{inter}}^{(0)}(\vec{q}, \omega) = \frac{A}{4\pi^2} \int d^2\vec{k} \times \left(\frac{\Theta(k_F - k)}{\hbar\omega - (\epsilon_{\vec{k}} + \epsilon_{\vec{k}+\vec{q}}) + i0^+} - \frac{1}{\hbar\omega - (\epsilon_{\vec{k}+\vec{q}} + \epsilon_{\vec{k}}) + i0^+} \right). \quad (11)$$

When working with the linearized low-energy theory, the limits are from 0 to k_c , where k_c is the momentum cutoff for the linearized theory, defined in such a way that the area of a model circular BZ with cone is equal to the original BZ: $\pi k_c^2 = A_{\text{BZ}} = 8\sqrt{3}\pi^2/(9a^2)$. Substituting the linear dispersion in polar coordinates, the inter-band part simplifies to,

$$\chi_{\text{inter}}^{(0)}(\vec{q}, \omega) = \frac{-A}{4\pi^2} \int_{k_F}^{k_c} k dk \int_0^{2\pi} d\phi \times \frac{1}{\hbar\omega - \hbar v_F (k + \sqrt{k^2 + q^2 + 2kq \cos \phi}) + i0^+}. \quad (12)$$

The imaginary and real part of the above $\chi_{\text{inter}}^{(0)}$ is calculated in the appendix. The final results we use in our plots are given by Equations (A10) and (A12) which are again valid for values of $|\vec{q}|$ which are small compared to k_F .

III. ANALYTIC AND NUMERICAL RESULTS

Within the RPA approximation, the dispersion of the neutral triplet collective mode can be seen as enhancement of the susceptibility given in Eq. (3). Since the $\chi_{\text{triplet}}^{\text{RPA}}$ is a retarded response satisfying the Kramers-Kronig relation, the imaginary (dissipative) part is identically zero in regions where the denominator of Eq. (3) might have zeros:

$$\Re \chi^{(0)}(\vec{q}, \omega) = \frac{1}{U}, \quad \Im \chi^{(0)}(\vec{q}, \omega) = 0. \quad (13)$$

As an alternative to solving the above equations, we give the contour plots of $\Re \chi_{\text{triplet}}^{\text{RPA}}$.

To make the comparison of the original theory (in the full BZ) with that of the linearized theory (one Dirac cone in a circular BZ), one needs to keep in mind that the values of U for the renormalized theory should be renormalized to the bandwidth $k_c v_F$. Also with the assumption of only one cone in the circular BZ, the kinetic energy the particle-hole processes occurring at each cone are underestimated by a factor of 2. Therefore when we compare a graph from the analytical result obtained for the linearized theory with a numerical result, one should keep in mind to properly interpret the value of analytical results according to $U \rightarrow 0.4548U$. For clarity, in figures related to analytical results, we have performed this conversion.

Fig. 2 shows the intensity plots of RPA triplet susceptibility for various values of U , using the analytic results of Equations (A6), (A8), (A10) and (A12). The doping is fixed by the value of chemical potential $\mu = 0.4$ eV. Fig. 3 on the other hand shows the same quantity obtained from numerical evaluation of the $\chi^{(0)}$ integral. The borders of the window outside

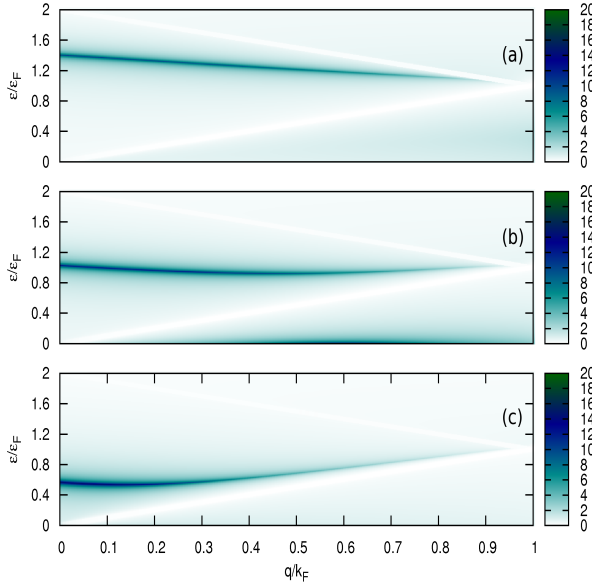


FIG. 2: (Color online) Contour plot for $\Re\chi_{\text{triplet}}^{\text{RPA}}$ using the analytic formulae obtained in Equations (A6), (A8), (A10) and (A12). The chemical potential is fixed at $\mu = 0.4$ eV. Different panels correspond to (a) $U=1.82t$, (b) $U=2.00t$, (c) $U=2.18t$. Borders of the triangular region of Fig. 1 (e) are shown in white here.

the particle-hole continuum where the collective mode can exist is denoted by white cuts in both figures. These figures are qualitatively similar. The precise shapes of the analytical and numerical dispersion are not expected to be identical³³. Because the numerical calculation takes the details of band structure e.g. curvatures and warping into account, while the analytical result is a *model* calculation assuming a circular BZ with one cone, where the kinetic energy part is assumed to have the form of a cone all over the circular BZ, without any curvature or warping.

In Figs. 4, 5 we plot the dispersion of collective mode using analytic and numerical results, respectively. In this figures, we change the doping level μ for fixed values of U . Again the figures are qualitatively similar.

As can be seen in Figs. 2, 3, 4 and 5, the neutral triplet collective mode in the small q region has essentially no dispersion and behaves as Einstein-like mode for the triplet particle-hole channel. For smaller values of U in Fig. 3, the collective mode is very close to the upper edge and is about to enter the PHC. With increasing the value of U , the electron-hole pairs are bound tighter into triplet packs, and hence the "binding energy" (measured from the upper edge of the PHC) increases. Near the limiting value of $U_c \sim 2.23t$, the triplet branch still exists in the gapful form and the gap does not vanish. Figures 4 and 5 show that the value of ω_{gap} very weakly decreases as one increases the μ in the range reported here. The behavior at very small μ will be different (see Eq. 16).

Finally in figure 6 we plot the $\Gamma - M$ cut in the BZ of the honeycomb lattice. Comparing this result with the one corresponding to undoped case, where the collective mode will be gapless at $\vec{q} = 0$ ^{16,17}, in doped case the intra-band levels

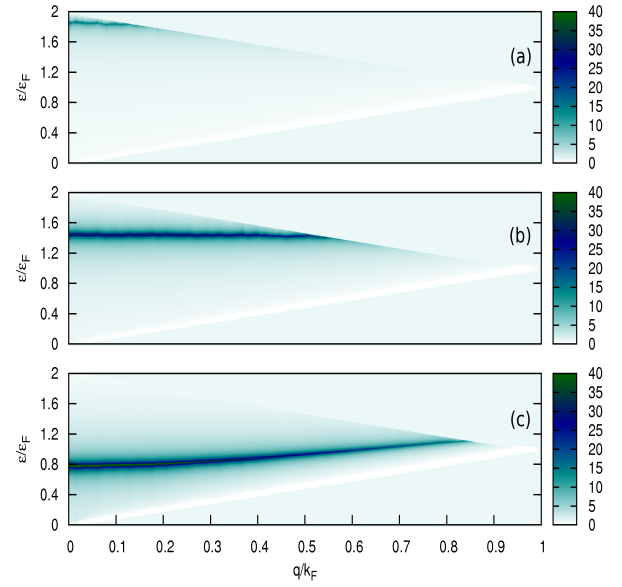


FIG. 3: (Color online) Numerical calculation of the spin-1 collective mode for (a) $U=1.8t$, (b) $U=2t$, (c) $U=2.2t$ and $\mu = 0.4$ eV. Borders of the triangular region of Fig. 1 (e) are shown in white here.

generated in the PHC push the small q part of the dispersion higher in energy, thereby making it gapful. The portion added to the PHC of undoped system is a 2D Fermi liquid-like part inside which the collective mode can not exist and gets Landau damped. The Einstein-like dispersion in the triangular window around the Γ point exists in the triangular window around the K point as well.

The gaped nature of spin-1 collective mode in the triangular window of the doped graphene is essentially a result of repulsion between the blue PHC states (Fig. 1 e). A simple asymptotic analysis of the contribution of these 2D like states with conic dispersion (unlike the quadratic dispersion of ordinary metals) gives $\Re\chi_{\text{intra}}^{(0)} \sim (\omega^2 - \hbar^2 v_F^2 q^2)^{-1/2}$ which is valid for small q , and arbitrary ω . When this asymptotic form inserted in Eq. (13) clearly gives a gap in the dispersion which tends to increase by increasing U . This indicates that the gap acquired by the neutral triplet collective mode is a result of repulsion of the PHC states arising from intra-band processes. However, note that as can be seen in Figs. 2, 3, the repulsion of the inter-band PHC states (denoted by cyan) dominates and the resultant trend of the gap is to decrease with increasing U . This should be contrasted to the 1D like phase space arising in the edge of the undoped PHC region which gives rise to a gapless dispersion of the collective mode¹⁷.

Our analytical results valid for the small q description of this collective mode enables us to find the behavior of the gap in the spectrum of this collective mode in terms of the doping parameters. To find the dependence of this "spin gap" to pa-

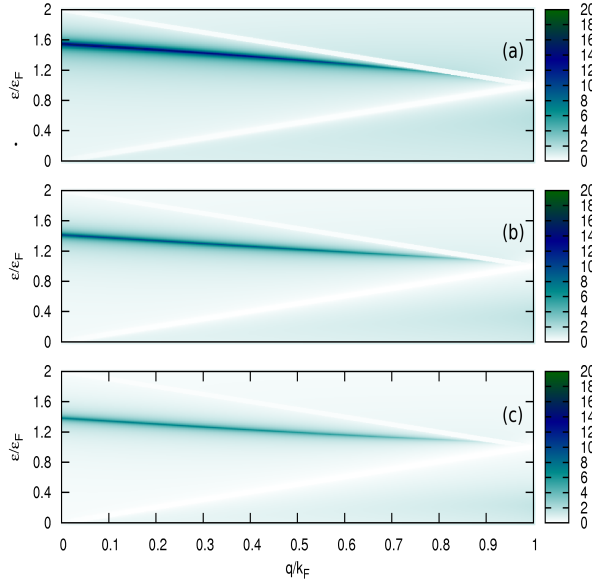


FIG. 4: (Color online) Analytic calculation of collective mode for (a) $\mu = 0.2$, (b) $\mu = 0.4$, (c) $\mu = 0.6$ eV and $U = 1.8t$. Borders of the triangular region of Fig. 1 (e) are shown in white here.

rameters, in $q \rightarrow 0$ limit we have:

$$\Re\chi_{\text{inter}}^{(0)}(\vec{q}, \omega) = \frac{A\hbar}{16\pi v_F^2} \times \left[4v_F(k_c - k_F) + 2\omega \ln\left(\frac{k_c}{k_F}\right) + 4qv_F + \omega q \left(\frac{1}{k_F} + \frac{1}{k_c}\right) \right], \quad (14)$$

which gives the following dispersion for the spin-1 collective mode:

$$\omega_{\text{spin}}(q) = \frac{B + \frac{4\mu}{v_F} - \frac{4q}{v_F}}{\frac{2}{v_F^2} \ln\left(\frac{\Lambda}{\mu}\right) + \hbar q v_F \left(\frac{1}{\mu} + \frac{1}{\Lambda}\right)}, \quad (15)$$

with $B = \frac{16\pi}{UA\hbar} - \frac{4k_c}{v_F}$ and $\Lambda = \hbar v_F k_c$. As can be seen the constants are such that the above dispersion can be linearized in q , in agreement with the density plots presented earlier. To obtain the spin gap magnitude, we set $\vec{q} = 0$ in the above formula to obtain:

$$\omega_{\text{gap}} = \frac{\left(\frac{16\pi}{UA\hbar} - \frac{4k_c}{v_F}\right) v_F^2 + 4\mu}{2 \ln\left(\frac{\Lambda}{\mu}\right)}. \quad (16)$$

Since the doping level μ can be most conveniently controlled by gate voltages, this formula can have experimental consequences. One can see that the above gap vanishes in the $\mu \rightarrow 0$ limit corresponding to the undoped case, in agreement with our earlier finding¹⁷. For very small values of doping, $\mu \ll t$, the characteristic inverse logarithmic dependence of the spin gap dominates. This suggests that optical spectroscopies with polarized radiation are likely to help in tracing the location of bound state in order to examine the peculiar inverse logarithmic μ dependence in our formula.

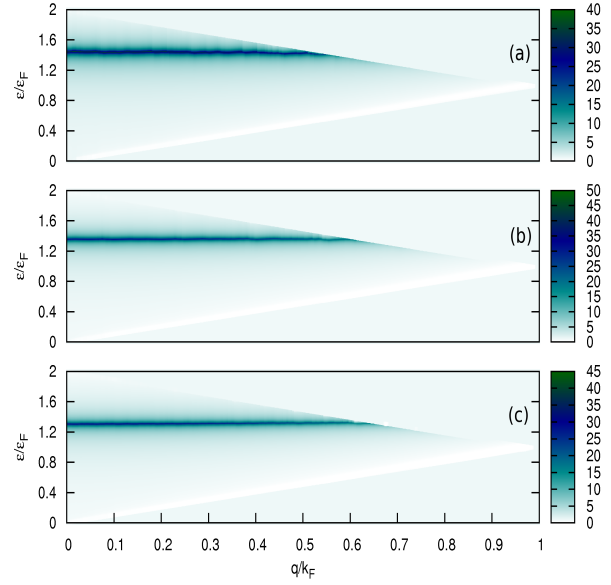


FIG. 5: (Color online) Numerical calculation of collective mode for (a) $\mu = 0.4$, (b) $\mu = 0.5$, (c) $\mu = 0.6$ eV and $U = 2t$. Borders of the triangular region of Fig. 1 (e) are shown in white here.

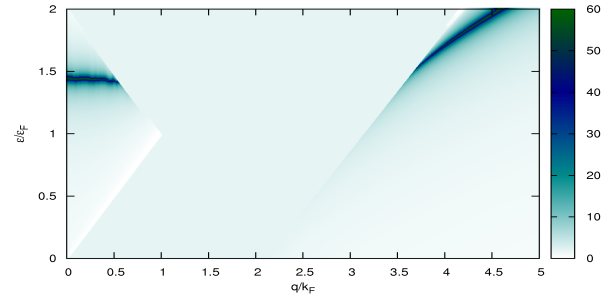


FIG. 6: (Color online) Numerical calculation of collective mode for $U = 2t$ and $\mu = 0.4$ eV along $\Gamma - M$ direction of the Brillouin zone. The PHC is more clear in Fig. 1 (c).

IV. SUMMARY AND DISCUSSION

We investigated the dispersion of the triplet neutral collective mode which was predicted to exist in undoped Dirac liquids¹⁶ in presence of doping. Populating the conduction band of the Dirac cone generates new levels in the PHC which repel the triplet bound state and make it gapful via a genuine inverse logarithmic dependence on the chemical potential. This new portion added to the PHC also causes Landau damping of some parts of the neutral triplet collective mode as compared to the undoped case.

Such triplet collective modes are characteristic of Dirac liquids, as opposed to ordinary metallic states with extended Fermi surface. In the Dirac cone case, there will be windows below the PHC near to Γ and K points, with no free particle-hole pairs allowed. These windows provide the essential phase space for the formation of a gapped triplet particle-hole pair.

This bound state for the undoped case was interpreted as a two-spinon bound state on top of a long range RVB ground state^{16,28}. For small values of doping where this RVB picture²⁸ can be assumed to prevail by continuity, the gaped nature of such collective mode can be interpreted as a new RVB state with shorter bonds. It would be interesting experimental question to search for this inverse-logarithmic dependence of the bound state energy. This also suggests a genuine way shortening the valence bonds by "screening" the bonds.

Development of short range singlet correlations in zero momentum channel in a conductor is synonymous to development of superconducting correlations. In an independent variational study, using the same repulsive Hubbard model that we have used, Pathak and collaborators have found superconductivity in graphene, for a range of doping. At an optimal doping they have predicted high temperature (Kosterlitz type) superconductivity. We interpret our spin-1 collective mode as signalling growth of short range spin singlet correlation in the ground state. Further, in a self consistent theory, our spin-1 collective mode should modify the metallic ground state and become the spin-1 collective mode of the superconducting ground state.

V. ACKNOWLEDGEMENTS

We thank K. Haghighi for technical assistance in computing facilities. S.A.J. was supported by the Vice Chancellor for Research Affairs of the Isfahan University of Technology, and the National Elite Foundation (NEF) of Iran.

APPENDIX A: ANALYTIC EVALUATION OF INTEGRALS FOR THE LOW-ENERGY THEORY

Let us calculate the integrals needed in Eqs. (9,12).

1. Intra-band term

Using the formula $\frac{1}{x+i0^+} = P\frac{1}{x} - i\pi\delta(x)$, the imaginary part can be most conveniently written as,

$$\begin{aligned} \Im\chi_{\text{intra}}^{(0)}(\vec{q}, \omega) = & \\ & -\frac{A}{4\pi^2} \int d^2\vec{k} \left[\delta(\hbar\omega - \epsilon_{\vec{k}} + \epsilon_{\vec{k}+\vec{q}}) - \delta(\hbar\omega + \epsilon_{\vec{k}} - \epsilon_{\vec{k}+\vec{q}}) \right] = \\ & -\frac{A}{4\pi^2} \int_0^{k_F} k dk \int_0^{2\pi} d\phi \left[\delta(z - k + \sqrt{k^2 + q^2 + 2kq \cos \phi}) \right. \\ & \left. - \delta(z + k - \sqrt{k^2 + q^2 + 2kq \cos \phi}) \right], \end{aligned} \quad (\text{A1})$$

where $z = \omega/v_F$. The delta integrals are simplified by using the formula $\delta(f(x)) = \sum_s \frac{\delta(x-s)}{|\nabla_x f(x)|_{x=s}}$ where s is a root of $f(x)$. Let us define,

$$f(k, q, \phi) = z \pm (k - \sqrt{k^2 + q^2 + 2kq \cos \phi}). \quad (\text{A2})$$

In term of new variable $u = \cos \phi$, the root of $f(k, q, \phi) = 0$ is, $u = \frac{z^2 - q^2 \pm 2zq}{2kq}$, which gives

$$\nabla_u f(k, q, u) = -\frac{kq}{z \pm k} \quad (\text{A3})$$

Substituting,

$$d\phi = -\frac{du}{\sqrt{1-u^2}}, \quad (\text{A4})$$

in Eq. (A1) the u integral becomes trivial and we are left with the following integration over the radial variable k :

$$\begin{aligned} \Im\chi_{\text{intra}}^{(0)}(\vec{q}, z) = & \frac{-A}{2\pi\hbar v_F} \int_0^{k_F} dk \times \\ & \left(\frac{(k-z)\Theta(k - \frac{z+q}{2})}{q\sqrt{1 - (\frac{z^2 - q^2 - 2zk}{2kq})^2}} - \frac{(k+z)\Theta(k - \frac{q-z}{2})}{q\sqrt{1 - (\frac{z^2 - q^2 + 2zk}{2kq})^2}} \right) \end{aligned} \quad (\text{A5})$$

The step functions in integrand correspond to the particle-hole (p-h) continuum. We restrict ourselves to the $q < 2k_F$ region. In this region, the dissipative part of intra-band processes is non-zero only when $\omega < qv_F$. The radial integration can be performed to give^{34,35},

$$\begin{aligned}
\Im\chi_{\text{intra}}^{(0)}(\vec{q}, z) = & \\
\frac{-A}{16\pi\hbar v_F} \frac{q}{\sqrt{1-z^2/q^2}} & \left[\left(1 - 2\frac{z^2}{q^2}\right) \ln \left(\left(\frac{2k_F - z}{q}\right) + \sqrt{\left(\frac{2k_F - z}{q}\right)^2 - 1} \right) + \left(\frac{2k_F - z}{q}\right) \sqrt{\left(\frac{2k_F - z}{q}\right)^2 - 1} \right. \\
& \left. - \left(1 - 2\frac{z^2}{q^2}\right) \ln \left(\left(\frac{2k_F + z}{q}\right) + \sqrt{\left(\frac{2k_F + z}{q}\right)^2 - 1} \right) - \left(\frac{2k_F + z}{q}\right) \sqrt{\left(\frac{2k_F + z}{q}\right)^2 - 1} \right] \quad (\text{A6})
\end{aligned}$$

For calculation of $\Re\chi_{\text{intra}}^{(0)}(\vec{q}, \omega)$, we directly use Eq. (5) and we find:

$$\begin{aligned}
\Re\chi_{\text{intra}}^{(0)}(\vec{q}, z) &= \frac{A}{4\pi^2\hbar v_F} \int d^2\vec{k} \left[\frac{1}{z - k + \sqrt{k^2 + q^2 + 2kq \cos \phi}} - \frac{1}{z + k - \sqrt{k^2 + q^2 + 2kq \cos \phi}} \right] \\
&= \frac{A}{2\pi^2\hbar v_F} \int_0^{k_F} k dk \int_{-\pi}^{\pi} d\phi \frac{k - \sqrt{k^2 + q^2 - 2kq \cos \phi}}{z^2 - (k - \sqrt{k^2 + q^2 - 2kq \cos \phi})^2}. \quad (\text{A7})
\end{aligned}$$

The ϕ integral can be evaluated and simplified to give,

$$\begin{aligned}
\Re\chi_{\text{intra}}^{(0)}(\vec{q}, z)|_{z>q} &= \frac{A}{\pi\hbar v_F} \int_0^{k_F} dk \times \\
& \left(\frac{k(z-k)}{\sqrt{[(q-k)^2 + (z-k)^2][(q+k)^2 - (z-k)^2]}} - \frac{k(z+k)}{\sqrt{[(z+k)^2 - (q-k)^2][(z+k)^2 - (q+k)^2]}} \right) \\
&= \frac{A}{16\pi\hbar v_F} \frac{1}{\sqrt{z^2 - q^2}} \times \left[(q^2 - 2z^2) \ln \left(\left(\frac{2k_F + z}{q}\right) + \sqrt{\left(\frac{2k_F + z}{q}\right)^2 - 1} \right) \right. \\
& - (q^2 - 2z^2) \ln \left(\left(\frac{2k_F - z}{q}\right) + \sqrt{\left(\frac{2k_F - z}{q}\right)^2 - 1} \right) - (q^2 - 2z^2) \ln \left(\left(\frac{z}{q}\right) + \sqrt{\left(\frac{z}{q}\right)^2 - 1} \right) \\
& \left. - (q^2 - 2z^2) \ln \left(-\left(\frac{z}{q}\right) + \sqrt{\left(\frac{z}{q}\right)^2 - 1} \right) - q^2 \left(\frac{2k_F - z}{q}\right) \sqrt{\left(\frac{2k_F - z}{q}\right)^2 - 1} + q^2 \left(\frac{2k_F + z}{q}\right) \sqrt{\left(\frac{2k_F + z}{q}\right)^2 - 1} \right]. \quad (\text{A8})
\end{aligned}$$

Demanding the expressions under square root to be positive, gives the following region for the window protected from the particle-hole energy levels: $q < z < -q + 2k_F$.

2. Inter-band term

Starting from Eq. (12), the imaginary part of $\chi_{\text{inter}}^{(0)}$ can be written as,

$$\Im\chi_{\text{inter}}^{(0)}(\vec{q}, z) = \frac{A}{4\pi v_F} \int_{k_F}^{k_c} k dk \int_0^{2\pi} d\phi \delta \left(z - k - \sqrt{k^2 + q^2 + 2kq \cos \phi} \right) \quad (\text{A9})$$

First we do integration on ϕ , and we find¹⁷:

$$\begin{aligned}
\Im\chi_{\text{inter}}^{(0)}(\vec{q}, z) &= \frac{A}{2\pi\hbar v_F} \int_{k_F}^{k_c} dk \frac{z-k}{q\sqrt{1 - \left(\frac{z^2 - q^2 - 2zk}{2kq}\right)^2}} \left[\Theta \left(k - \frac{z+q}{2} \right) - \Theta \left(\frac{z-q}{2} - k \right) \right] \\
&= \frac{A}{16\hbar v_F} \frac{2z^2 - q^2}{\sqrt{z^2 - q^2}}, \quad -q + 2k_F < z < q + 2k_c \quad (\text{A10})
\end{aligned}$$

Now we use Kramers-Kronig relation for calculation of $\Re\chi_{\text{inter}}^{(0)}$ from imaginary part, $\chi_{\text{inter}}^{(0)}$ ¹⁷:

$$\Re\chi_{\text{inter}}^{(0)}(\vec{q}, \omega) = \frac{A}{16\pi\hbar v_F^2} \int_{(-q+2k_F)v_F}^{(q+2k_c)v_F} \frac{d\omega'}{\omega' - \omega} \frac{2\omega^2 - q^2 v_F^2}{\sqrt{\omega^2 - q^2 v_F^2}}. \quad (\text{A11})$$

Defining the new variable η by the relation $\omega' = qv_F \coth(\eta)$, the limits of integration η_1, η_2 are given by $\coth(\eta_2) = 1 + 2k_c/q$, $\coth(\eta_1) = -1 + 2k_F/q$, so that we obtain:

$$\begin{aligned} \Re\chi_{\text{inter}}^{(0)}(\vec{q}, \omega) &= \frac{Aq^2}{16\pi\hbar} \int_{\eta_1}^{\eta_2} d\eta \frac{2 \coth^2(\eta) - 1}{\sinh(\eta) [\omega - qv_F \coth(\eta)]} \\ &= \frac{A}{16\pi\hbar} \left\{ \frac{-q}{v_F} \left(2 + 2\frac{k_c - k_F}{q} + \frac{2k_F}{q} \sqrt{1 - \frac{q}{k_F}} - \frac{2k_c}{q} \sqrt{1 + \frac{q}{k_c}} \right) - \frac{2\omega}{v_F^2} \ln \left(\frac{-1 + \frac{2k_F}{q} - \frac{2k_F}{q} \sqrt{1 - \frac{q}{k_F}}}{1 + \frac{2k_c}{q} - \frac{2k_c}{q} \sqrt{1 + \frac{q}{k_c}}} \right) \right. \\ &\quad + \frac{2q^2(1 - 2\omega^2/v_F^2)}{\sqrt{q^2v_F^2 - \omega^2}} \left[\arctan \left(\frac{qv_F(1 + \frac{2k_c}{q} - \frac{2k_c}{q} \sqrt{1 + \frac{q}{k_c}}) - \omega}{\sqrt{q^2v_F^2 - \omega^2}} \right) - \arctan \left(\frac{qv_F(-1 + \frac{2k_F}{q} - \frac{2k_F}{q} \sqrt{1 + \frac{q}{k_F}}) - \omega}{\sqrt{q^2v_F^2 - \omega^2}} \right) \right] \\ &\quad \left. + \frac{q}{v_F(1 + \frac{2k_c}{q} - \frac{2k_c}{q} \sqrt{1 + \frac{q}{k_c}})} - \frac{q}{v_F(-1 + \frac{2k_F}{q} - \frac{2k_F}{q} \sqrt{1 + \frac{q}{k_F}})} \right\}. \end{aligned} \quad (\text{A12})$$

Equations (A6), (A8), (A10) and (A12) complete the analytic evaluation of the total non-interacting susceptibility $\chi^{(0)} = \chi_{\text{intra}}^{(0)} + \chi_{\text{inter}}^{(0)}$

-
- ¹ K.S. Novoselov, A.K. Geim, S.V. Morozov, D. Jiang, Y. Zhang, S.V. Dubonos, I.V. Grigorieva, and A.A. Firsov, *Science* **306**, 666 (2004); K.S. Novoselov, A.K. Geim, S.V. Morozov, D. Jiang, M.I. Katsnelson, I.V. Grigorieva, S.V. Dubonos, A.A. Firsov, *Nature* **438**, 197 (2005).
- ² A. Bostwick, T. Ohta, T. Seyller, K. Horn, and E. Rotenberg, *Nature Physics* **3**, 36 (2007).
- ³ A. Bostwick, T. Ohta, J. L. McChesney, T. Seyller, K. Horn, E. Rotenberg, *solid state communications*, **143**, 63 (2007).
- ⁴ For a review see: A. H. Castro Neto, F. Guinea, N. M. R. Peres, K. S. Novoselov, A. K. Geim, *Rev. Mod. Phys.* **81**, 109 (2009).
- ⁵ M. Amini, S. A. Jafari, F. Shahbazi, to appear in *Eur. Phys. Lett* (2009).
- ⁶ S. A. Jafari, *Eur. Phys. Jour. B*, **68**, 537 (2009).
- ⁷ Ben Yu-Kuang Hu, E. H. Hwang, S. Das Sarma, *Phys. Rev. B* **78**, 165411 (2008).
- ⁸ A. Qaiumzadeh, N. Arabchi, R. Asgari, *Solid State Commun.*, **147**, 172 (2008).
- ⁹ A. Garg, M. Randeria, N. Trivedi, APS March Meeting, 2007, abstract no. L8.006, cond-mat/0609666.
- ¹⁰ K. S. Novoselov, Z. Jiang, Y. Zhang, S. V. Morozov, H. L. Stormer, U. Zeitler, J. C. Maan, G. S. Boebinger, P. Kim and A. K. Geim, *Science* **315**, 1379 (2007).
- ¹¹ C. Berger, Z. Song, X. Li, X. Wu, N. Brown, C. Naud, D. Mayou, T. Li, J. Hass, A. N. Marchenkov, E. H. Conard, P. N. Firs, and W. A. de Heer, *Science* **312**, 1191 (2006).
- ¹² P. R. Wallace, *Phys. Rev.* **71**, 622 (1947).
- ¹³ S.Y. Zhou, G.-H. Gweon, J. Graf, A.V. Fedorov, C.D. Spataru, R.D. Diehl, Y. Kopelevich, D.-H. Lee, Steven G. Louie, A. Lanzara, *Nat. Phys.* **2**, 595 (2006).
- ¹⁴ G. Li, E. Y. Anderi, *Nat. Phys.* **3**, 623 (2007).
- ¹⁵ M. Orlita, C. Faugeras, G. Martinez, D. K. Maude, M. L. Sadowski, M. Potemski, *Phys. Rev. Lett.* **100** 136403 (2008).
- ¹⁶ G. Baskaran, S.A. Jafari, *Phys. Rev. Lett.* **89**, 016402 (2002); G. Baskaran, S.A. Jafari, *Phys. Rev. Lett.* **92**, 199702 (2004); N. M. R. Peres, M. A. N. Araujo, and A. H. Castro Neto, *Phys. Rev. Lett.* **92**, 199701 (2004).
- ¹⁷ S. A. Jafari and G. Baskaran, *Eur. Phys. J. B.* **43**, 175 (2005).
- ¹⁸ M. Ebrahimkhas, S. A. Jafari, *Phys. Rev. B*, bf 79, 205425 (2009).
- ¹⁹ I. Luk'yanchuk, Y. Kopelevich, M. El Marssi, *Physica B* **404** 404 (2009).
- ²⁰ M. Sprinkle, D. Siegel, Y. Hu, J. Hicks, P. Soukiassian, A. Tejada, A. Taleb-Ibrahimi, P. Le Fevre, F. Bertran, C. Berger, W.A. de Heer, A. Lanzara, E.H. Conrad, arXiv:0907.5222.
- ²¹ L. Pauling, *Nature of The Chemical Bond*, Cornell University Press, NY, (1960).
- ²² G. Baskaran, *Phys. Rev. B* **65**, 212505 (2002).
- ²³ A. M. Black-Schaffer, S. Doniach, *Phys. Rev. B* **75**, 134512 (2007).
- ²⁴ S. Pathak, V.B. Shenoy, G. Baskaran, arXiv:0809.0244v1
- ²⁵ P. Sahebsara, D. Senechal, arXiv:0908.0474v1.
- ²⁶ B. Uchoa, A. H. Castro Neto, *Phys. Rev. Lett.* **98**, 146801 (2007).
- ²⁷ C. Honerkamp, *Phys. Rev. Lett.* **100**, 146404 (2008).
- ²⁸ Z. Noorbakhsh, F. Shahbazi, S. A. Jafari and G. Baskaran, *J. Phys. Soc. Jpn.* **78**, 054701 (2009).
- ²⁹ J. E. Drut, and T. A. Lahde, *Phys. Rev. Lett.* **102**, 026802 (2009); J. E. Drut and T. A. Lahde, *Phys. Rev. B* **79**, 165425 (2009).
- ³⁰ G. Giovannetti, P. A. Khomyakov, G. Brocks, V. M. Karpan, J. van den Brink, and P. J. Kelly, *Phys. Rev. Lett.* **101**, 026803 (2008).
- ³¹ N. Nagaosa, *Quantum Field Theory in Condensed Matter Physics*, Springer-Verlag, Berlin, 1999.
- ³² N. E. Bickers, D. J. Scalapino, *Ann. Phys.* **193**, 206 (1989).
- ³³ A. Hill, S. A. Mikhailov and K. Zeigler, arXiv: 0904.4378.
- ³⁴ M. Abramowitz, I. A. Stegun, 1972, *Handbook of Mathematical Functions* (New York: Dover)
- ³⁵ B. Wunsch, T. Stauber, F. Sols, F. Guinea, *New. J. Phys.* **8**, 318 (2006).